molbank

MDPI

Short Note

2*S*-(1*RS*-benzyloxy-hex-5-enyl)-2,3-dihydro-1,4-benzodioxine

Angelica Artasensi and Laura Fumagalli *

Department of Pharmaceutical Sciences, University of Milan, 20133 Milan, Italy; angelica.artasensi@unimi.it
* Correspondence: laura.fumagalli@unimi.it

Abstract: In medicinal chemistry, the precise configuration of molecules is a crucial determinant of their pharmacological properties. Hence, the introduction of a new chiral center during the synthetic pathway involves the assignment of configuration. Herein we assign, by means of molecular modeling ^{1}H and 2D Nuclear Overhauser Effect NMR techniques, the configuration of the two diastereomers 2*S*-(1*R*-benzyloxy-hex-5-enyl)-2,3-dihydro-1,4-benzodioxine and 2*S*-(1*S*-benzyloxy-hex-5-enyl)-2,3-dihydro-1,4-benzodioxine, which are useful to synthetize analogs of the potent and highly selective dipeptidyl peptidase IV and carbonic anhydrase inhibitor recently published.

Keywords: NMR; stereocenter; molecular modeling; NOESY; benzodioxine; configuration

1. Introduction

The 2,3-dihydro-1,4-benzodioxine or benzo-1,4-dioxane substructure is a chemical motif that has garnered significant attention in the field of medicinal chemistry due to its presence in various drugs and drug candidates. The 2,3-dihydrobenzodioxine substructure's versatility stems from its ability to interact with specific biological receptors and enzymes, influencing cellular pathways in a targeted manner. This has led to the exploration of diverse chemical derivatives and analogs to fine-tune the pharmacological properties of compounds containing this motif [1–6]. This distinctive structural element, characterized by a six-membered ring fused with a benzene ring and an oxygen bridge, imparts unique pharmacological properties to the compounds that incorporate it. Nevertheless, the presence of chiral carbon on the skeleton and on other substructures of the molecule presents the possibility of having multiple stereoisomers and implies the assignment of the configuration.

In medicinal chemistry, the precise configuration of molecules is a crucial determinant of their pharmacological properties. Thus, determining the spatial arrangement of substituents around a chiral carbon holds great importance in understanding and optimizing the therapeutic potential of drugs. This process is so important that subtle changes in molecular structure could drastically impact on the efficacy, safety, and pharmacokinetics of a compound. As a matter of fact, many approaches have been developed to obtain either pure enantiomers of molecules containing benzo-1,4-dioxane or to assign the correct configuration of chiral carbons comprised in molecules which include this skeleton [7,8]. Herein we report a synthetic strategy to obtain 2-(1-benzyloxy-hex-5-enyl)-2,3-dihydro-1,4-benzodioxine, which is useful to synthetize analogs of the potent and highly selective dipeptidyl peptidase IV and carbonic anhydrase inhibitor recently published [9]. Moreover, the characterization of all the intermediates is described, and the configuration of the final product is assigned by means of molecular modeling ^{1}H and 2D Nuclear Overhauser Effect NMR (NOESY) techniques. In addition, a modified Karplus equation was applied to corroborate the experimental data [10,11].

check for updates

Citation: Artasensi, A.; Fumagalli, L. 2*S*-(1*RS*-benzyloxy-hex-5-enyl)-2,3-dihydro-1,4-benzodioxine. *Molbank* **2024**, *2024*, M1812. https://doi.org/10.3390/M1812

Academic Editor: Fawaz Aldabbagh

Received: 4 March 2024
Revised: 15 April 2024
Accepted: 17 April 2024
Published: 24 April 2024

Copyright: © 2024 by the authors. Licensee MDPI, Basel, Switzerland. This article is an open access article distributed under the terms and conditions of the Creative Commons Attribution (CC BY) license (https://creativecommons.org/licenses/by/4.0/).

2. Results and Discussion

Recently, we synthesized dipeptidyl peptidase IV and carbonic anhydrase inhibitors as a potential innovative approach for the simultaneous treatment of diabetes and obesity, namely diabesity [9].

In an attempt to synthesize new analogs characterized by a more flexible and variously functionalized linker between the two aromatic portions, we planned the synthetic strategy reported in Scheme 1.

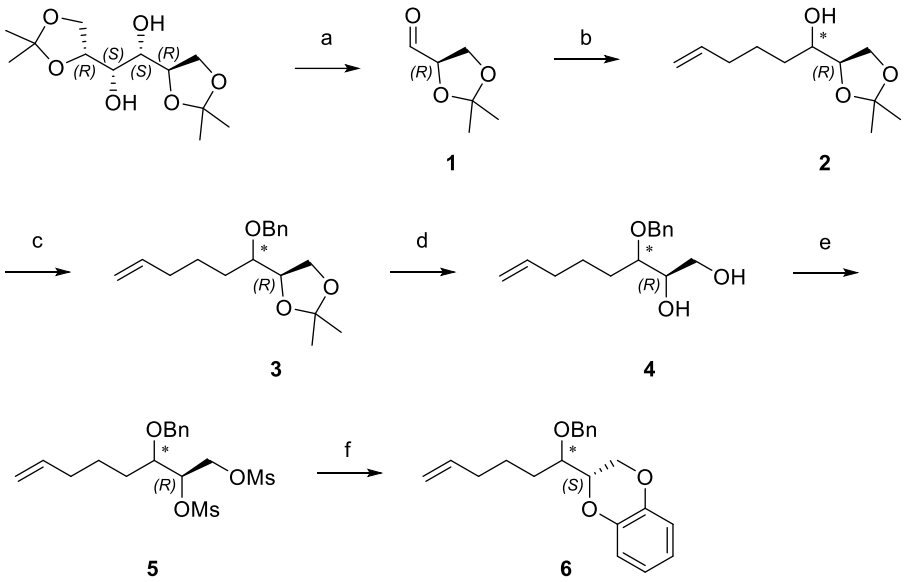

Scheme 1. Synthesis of 2-(1-benzyloxy-hex-5-enyl)-2,3-dihydro-1,4-benzodioxine (**6**). Reagents and conditions: (**a**) $NaHCO_3$ sat., $NaIO_4$, DCM, RT; (**b**) Mg, I_2, 5-bromopentene, THF, reflux; (**c**) NaH, BnBr, THF, RT; (**d**) HCl 10%, MeOH, RT; (**e**) TEA, MsCl, DCM, RT; (**f**) K_2CO_3, catechol, DMF, RT.

D-Mannitol diacetonide was cleaved via oxidation according to Schmid et al. [12]. Then, the alkyl chain was enlarged under a Grignard reaction with 4-pentenyl magnesium bromide, and a new stereo center was generated. The two diastereomers were maintained in the mixture for the subsequent synthetic steps. Nevertheless, since the different retention factors (R_f) on thin layer chromatography (TLC) made the separation possible, they were isolated by chromatography on silica gel, characterized by optical rotation and ^{1}H-NMR, and afterwards reunited. (2*R*,3*RS*)-1,2-isopropylidenedioxy-7-octen-3-ol (**2**), after having been benzylated (**3**), underwent acidic acetal hydrolysis to furnish vicinal diol (**4**), which was mesylated (**5**).

(2*R*,3*RS*)-1,2-mesyloxy-7-octen-3-benzyloxy (**5**) reacted with catechol in basic condition to give 2*S*-(1*RS*-benzyloxy-hex-5-enyl)-2,3-dihydro-1,4-benzodioxine (**6**). At this stage, since the benzo-1,4-dioxane skeleton had been built, we isolated the two diastereomers with the intention of assigning the corresponding configuration to carbon 1′ (Figure 1 numbers in green) of the alkyl chain by means of molecular modeling ^{1}H and 2D-NOESY NMR analyses.

NOESY provides connectivity based on the Nuclear Overhauser Effect (NOE), which alters signal intensity on a direct through-space mechanism that is distance dependent. Thus, the experiment can be exploited to assign spatial configuration considering internuclear distances.

First of all, we chose deuterated benzene (C_6D_6) as the most suitable deuterated solvent in order to reach the best resolution of the peaks related to the interested protons, namely 2H and 1′H (Figure 1B; to compare the resolution refer to Figures S5, S6, S9, and S10 of the Supplementary Materials). From the ^{1}H-NMR spectra of the two diastereomers, this proton (2H, Figure 1B) linked to 2C chiral carbon (Figure 1A) belonging to the benzodioxane

skeleton, which was maintained in *S* configuration, is at 4.0 and 4.16 ppm, while the 1′H linked to 1′C (the new stereo center resulting from the Grignard reaction) is at 3.6 and 3.52 ppm, respectively. In addition, the diastereomer characterized by the proton of a new stereocenter at 3.6 ppm showed the highest R_f on TLC. The coupling constant between 1′H and 2H is 12.8 Hz for the diastereomer with higher R_f, while, for the other, this is 4.8 Hz. Moreover, from the comparison of the ^{1}H-NMR spectra, only the diastereomer with lower R_f shows a more complex pattern of signal related to proton 2H, giving evidence for a different spatial orientation. Nevertheless, these differences in chemical shifts, coupling constants, and shapes are not enough to assign the configuration to 1′C.

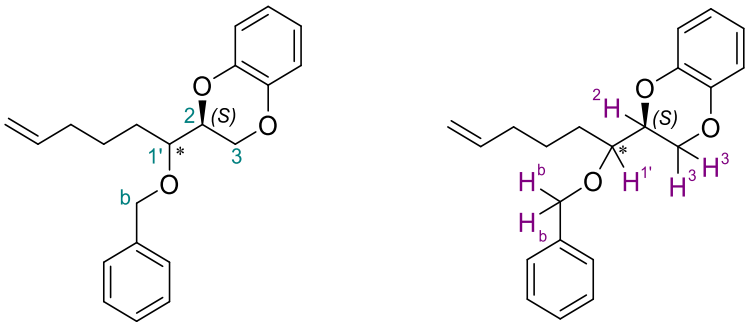

Figure 1. Numbering of the interested carbons and protons panels (**A**) and (**B**), respectively.

The 1′H-C-C-2H coupling constant depends on the dihedral angle between the associated C-H bonds; dihedral angles of close to 180° (antiperiplanar) give rise to the largest couplings, and dihedral angles of close to 0° (synperiplanar) also give rise to significant couplings. Close to 30° dihedral angles (gauche) result in lesser couplings; close to 90° dihedral angles yield close to 0 Hz coupling constants, which are frequently not encountered. Thus, we exploited molecular modeling and Karplus relationships to predict the coupling constants to be compared to the experimental ones.

The molecular modeling analyses show that the diastereomer *SR* (Figure 2A) adopts an antiperiplanar disposal with a 179.18° dihedral angle (Figure 2B), while the diastereomer *SS* (Figure 2C) assumes a gauche disposition with a 62.49° dihedral angle (Figure 2D).

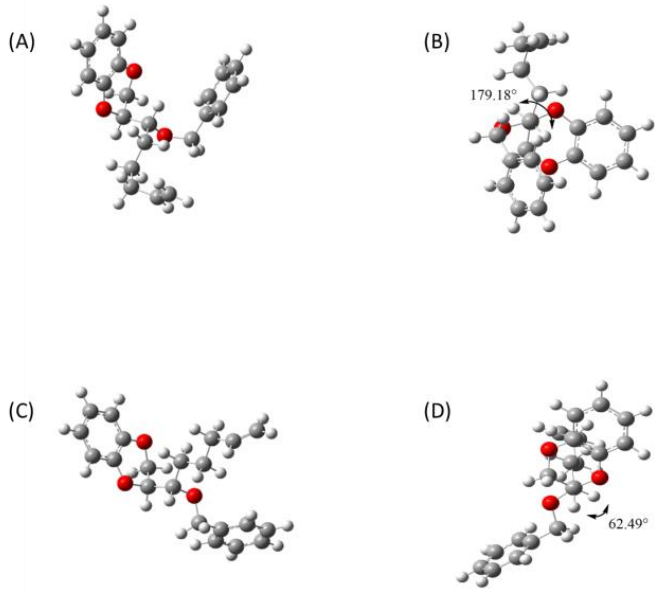

Figure 2. Molecular models with dihedral angle of diastereomer *SR* panels (**A**,**B**) and diastereomer *SS* panels (**C**,**D**).

From these data, the predicted coupling constants resulted from the application of the modified Karplus Equation (1) of the diastereomers are 11.89 Hz for the *SR* and 4.54 Hz for the *SS*, respectively, which are in line with the ones experimentally obtained [10,11,13].

$$J/\mathrm{Hz} = 7 - \cos\theta + 5\cos 2\theta \quad (1)$$

To confirm the hypothesized configuration, we performed a 2D-NOESY experiment.

2D-NOESY provides information about spatial closeness of protons that are separated by up to about 5 Å. Hence, this is the most direct way to assign the configuration to the 1′C by considering the relationship of its proton 1′H to neighboring protons in 3D space (via their dihedral torsion angle and coupling constant) and combining this with the 2D-NOESY spectrum.

The 2D-NOESY spectrum of the diastereomer with higher R_f (Figure 3) clearly shows a significant correlation between the 1′H proton (3.6 ppm) of the new chiral center, the chiral proton of the benzodioxane skeleton, the 3H protons of the benzodioxane ring, and the two benzylic protons.

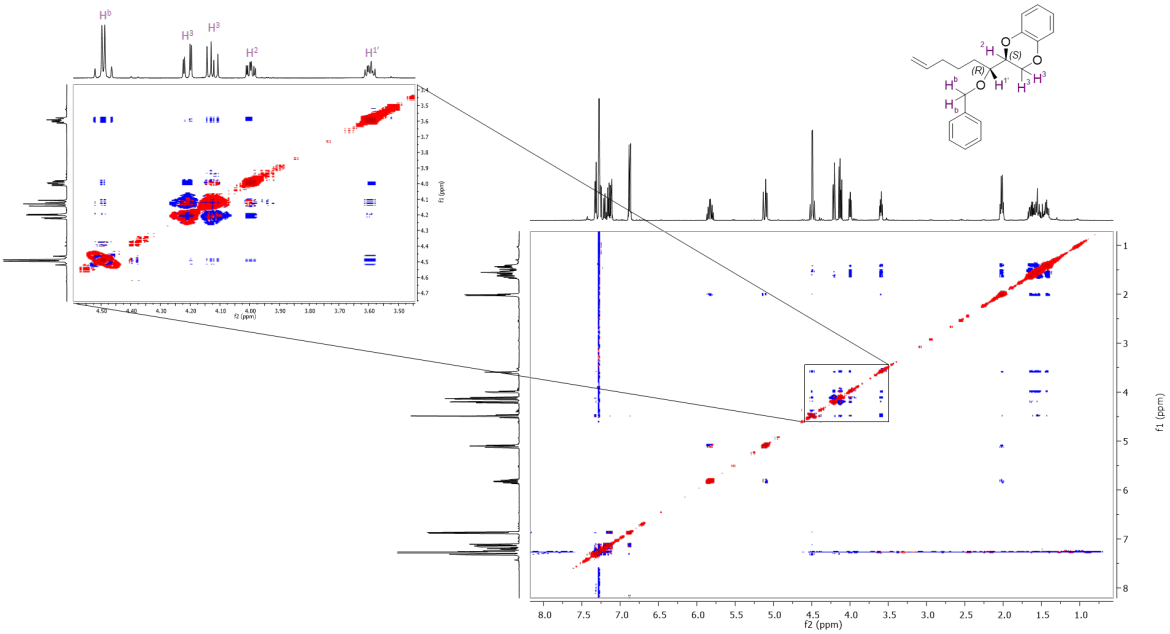

Figure 3. The 2D-NOESY spectrum of the diastereomer with R_f = 0.63.

Conversely, the 2D-NOESY spectrum of the diastereomer with lower R_f (Figure 4) shows a correlation between the 1′H proton (3.52 ppm) of the new chiral center, the chiral proton of the benzodioxane skeleton and the two benzylic protons, but there is no cross peak with 3H protons, indicating that the 1′H proton is more distant. Furthermore, the distances of the 1′H to 3H protons are 2.95 Å and 3.78 Å for the *R* configuration, which justify the good correlation showed by the 2D-NOESY of the diastereomer with a higher R_f and 3.77 Å and 4.28 Å for the *S* configuration that validates the absent correlation between 1′H proton and 3H protons in the 2D-NOESY of the other diastereomer (for distances, refer to Figures S7 and S8 of the Supplementary Materials). Hence, we were able to assign the *R* configuration to the diastereomer with higher R_f (0.63) and *S* configuration to the one with lower R_f (0.54).

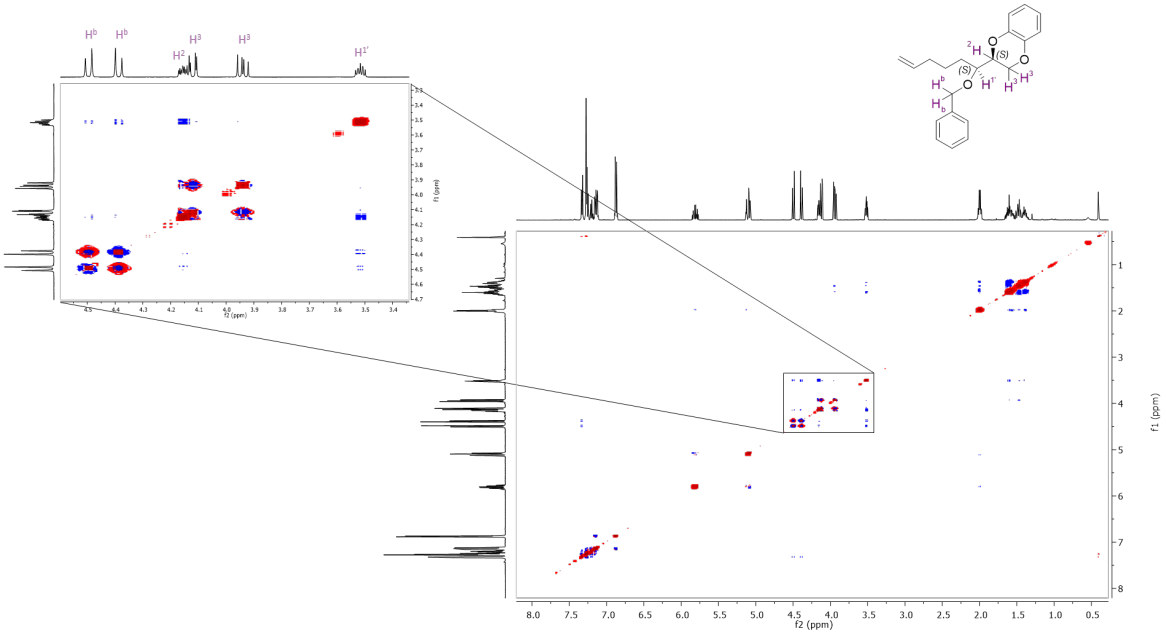

Figure 4. The 2D-NOESY spectrum of the diastereomer with R_f = 0.54.

3. Materials and Methods

All reagents and solvents were purchased by Merck KGaA, Darmstadt, Germany and used as received. The purification of all compounds was performed on Biotage® Isolera (Biotage Sweden AB, Uppsala, Sweden) using Sfär silica D 60. The retention factors (R_f) were calculated using Supelco TLC cards with fluorescent indicator 254 nm. A Jasco P-1010 polarimeter (Perkin Elmer, Waltham, USA) was used to determine optical rotations. The ^{1}H and 2D-NOESY NMR spectra were recorded at 500 MHz (Bruker Avance 500 Billerica, MA, USA) and processed by Mnova software. Chemical shifts are reported relative to residual solvents $CDCl_3$ or C_6D_6. The ^{1}H-NMR coupling constants (J) are reported in Hertz (Hz), and multiplicities are indicated as follows: s (singlet), d (doublet), dd (doublet of doublets), ddt (doublet of doublet of triplets), t (triplet), and m (multiplet), brs (broad signal).

Molecular modeling software: *Ab initio* Density Functional Theory (DFT) calculations were carried out using Gaussian 16; they were performed using the B3LYP-6-31+g(d,p) basis set. Distances between protons were measured on VEGA ZZ version 3.2.4. [14].

R-Glyceraldehyde acetonide (**1**)

Saturated aqueous $NaHCO_3$ (15 mL) was added to a solution of D-mannitol diacetonide (26.17 g, 99.7 mmol) in DCM (250 mL). Then, sodium metaperiodate (32.01 g, 149.66 mmol) was added in small portions. The resulting suspension was stirred for 45 min at room temperature. The mixture was stirred overnight until TLC indicated the disappearance of the starting material. Afterwards, the reaction was filtered, and the residue evaporated *in vacuo* to give the pure product **1** (24.80 g, 95.5%) as a yellow oil. TLC (cyclohexane/ethyl acetate 50:50) R_f = 0.39 ^{1}H NMR ($CDCl_3$) δ 9.72 (s, 1H), 4.49–4.32 (m, 1H), 4.26–4.00 (m, 2H), 1.48 (s, 3H), 1.42 (s, 3H). Since the product is a volatile compound, the evaporation pressure was set up to 40 mbar. $[\alpha]_D^{25}$ ($CHCl_3$, c = 1) + 39.21

(2R,3RS)-1,2-isopropylidenedioxy-7-octen-3-ol (**2**)

Under a nitrogen atmosphere, a solution of pentyl bromide (25 g, 167.74 mmol) in THF (80 mL) was added dropwise to a suspension of magnesium (4.08 g, 167.74 mmol) and catalytic iodine in dry THF (15 mL). The mixture was stirred under reflux for 2 h. Afterwards, a solution of **1** (24.80 g, 190.54 mol) in THF (20 mL) was added once the reaction mixture was ice-cooled. The mixture was kept stirred at room temperature overnight until TLC indicated the disappearance of the starting material. The reaction was quenched with a 10% aqueous solution of $NaHCO_3$, and the precipitate formed was filtered through a Celite® pad, while the organic layer was subsequently washed with 10% aqueous solution

of $NaHCO_3$ and brine. The organic phase was dried over anhydrous sodium sulfate, filtered, and evaporated in vacuo. Flash chromatography (cyclohexane/ethyl acetate 85:15) was performed to obtain the pure product **2** (both diastereomers, 26.71 g, 70.0%) as a yellow oil.

TLC (cyclohexane/ethyl acetate 85:15) R_f = 0.26, $[\alpha]_D^{25}$ ($CHCl_3$, c = 1) + 16.69, ^1H NMR ($CDCl_3$) δ 5.80 (ddt, *J* = 16.9, 10.1, 6.7 Hz, 1H), 5.06–4.93 (m, 2H), 4.05–3.95 (m, 2H), 3.73 (dd, *J* = 7.6, 6.1 Hz, 1H), 3.49 (m, 1H), 2.20 (d, *J* = 5.0 Hz, 1H), 2.15–2.03 (m, 2H), 1.70–1.60 (m, 2H), 1.49 (m, 1H), 1.44 (s, 4H), 1.37 (s, 3H).

TLC (cyclohexane/ethyl acetate 85:15) R_f = 0.22, $[\alpha]_D^{25}$ ($CHCl_3$, c = 1) + 14.65, ^1H NMR ($CDCl_3$) 5.80 (ddt, *J* = 16.9, 10.1, 6.7 Hz, 1H), 5.06–4.93 (m, 2H), 4.07–3.99 (m, 2H), 3.94 (td, *J* = 17.9, 6.3 Hz, 1H), 3.78 (m, 1H), 2.16–2.02 (m, 3H), 1.75 (brs, 1H), 1.63 (m, 1H), 1.53–1.44 (m, 2H), 1.43 (s, 3H), 1.37 (s, 3H).

(1RS,4R)-4-(1-(benzyloxy)hex-5-en-1-yl)-2,2-dimethyl-1,3-dioxolane (**3**)

Under a nitrogen atmosphere, a solution of **2** (26.71 g, 133.38 mmol) in THF (120 mL) was added dropwise to a suspension of NaH (3.52 g, 146.72 mmol) in THF (40 mL) and stirred for 30 min. Then, a solution of benzyl bromide (17.43 mL, 146.72 mmol) in THF (120 mL) was added to the reaction mixture, and it was stirred overnight until TLC indicated the disappearance of the starting material. Afterward, the mixture was diluted with DCM and washed with 10% aqueous solution of HCl and brine. The organic phase was dried over anhydrous sodium sulfate, filtered, and evaporated in vacuo, affording an orange oil. Flash chromatography (cyclohexane/ethyl acetate 95:5) was performed to obtain the pure product **3** (20.18 g, 52.10%) as a yellow oil.

TLC (cyclohexane/ethyl acetate 95:5) R_f = 0.36, $[\alpha]_D^{25}$ ($CHCl_3$, c = 1) + 8.38, ^1H NMR ($CDCl_3$) δ 7.41–7.27 (m, 5H), 5.79 (ddt, *J* = 16.9, 10.1, 6.6 Hz, 1H), 5.07–4.91 (m, 2H), 4.66 (d, *J* = 11.4 Hz, 1H), 4.59 (d, *J* = 11.4 Hz, 1H), 4.16–3.99 (m, 2H), 3.90 (dd, *J* = 7.7, 6.6 Hz, 1H), 3.54 (dd, *J* = 9.5, 5.8 Hz, 1H), 2.05 (dd, *J* = 12.6, 6.2 Hz, 2H), 1.65–1.44 (m, 4H), 1.42 (d, *J* = 0.6 Hz, 3H), 1.36 (s, 3H).

TLC (cyclohexane/ethyl acetate 95:5) R_f = 0.31 $[\alpha]_D^{25}$ ($CHCl_3$, c = 1) + 41.94, ^1H NMR ($CDCl_3$) δ 7.41–7.27 (m, 5H), 5.77 (ddt, *J* = 16.9, 10.2, 6.7 Hz, 1H), 5.05–4.89 (m, 2H), 4.77 (d, *J* = 11.7 Hz, 1H), 4.62 (d, *J* = 11.7 Hz, 1H), 4.21 (dd, *J* = 13.9, 6.6 Hz, 1H), 3.98 (dd, *J* = 8.2, 6.5 Hz, 1H), 3.74–3.63 (m, 1H), 3.49–3.35 (m, 1H), 2.02 (dd, *J* = 13.0, 6.4 Hz, 2H), 1.68–14.39 (m, 7H), 1.37 (s, 3H).

(2R,3RS)-3-(benzyloxy)oct-7-ene-1,2-diol (**4**)

10% aqueous solution of HCl (23 mL) was added to a solution of **3** (20.18 g, 69.49 mmol) in MeOH (230 mL). The reaction mixture was stirred at room temperature until TLC indicated the disappearance of the starting material. Afterwards, the solvent was evaporated in vacuo, and the residue was dissolved in DCM and water. The aqueous layer was further extracted two times with DCM. The reunited organic phases were washed with brine, dried over anhydrous sodium sulfate, and filtered. The solvent was evaporated in vacuo, providing the pure product **4** (16.7 g, 96.0%) as a yellow oil. TLC (cyclohexane/ethyl acetate 60:40) R_f = 0.16 ^1H NMR ($CDCl_3$) δ 7.44–7.27 (m, 5H), 5.80 (dt, *J* = 16.9, 6.7 Hz, 1H), 5.10–4.89 (m, 2H), 4.57 (m, 2H), 3.86–3.44 (m, 4H), 2.25 (brs, 2H), 2.08 (d, *J* = 6.5 Hz, 2H), 1.83–1.34 (m, 4H).

(2R,3RS)-3-(benzyloxy)-1,2-dimesiloxy-oct-7-ene (**5**)

Triethylamine (8.16 mL, 58.72 mmol) was added to a solution of **4** (7.00 g, 27.96 mmol) in DCM (50 mL). Then, after ice-cooling, mesyl chloride (4.54 mL, 58.72 mmol) was added dropwise. The mixture was stirred at room temperature until TLC indicated the disappearance of the starting material. Afterward, the reaction was diluted with dichloromethane, and the organic phase was washed with a 10% aqueous solution of HCl and then with brine. The organic phase was dried over anhydrous sodium sulfate and filtered, and the solvent was evaporated in vacuo, providing the pure product **5** (10.91 g, 82%) as a yellow oil. TLC (cyclohexane/ethyl acetate 50:50) R_f = 0.52 ^1H NMR ($CDCl_3$) δ 7.42–7.28 (m, 5H), 5.90–5.67 (m, 1H), 5.08–4.89 (m, 2H), 4.73–4.55 (m, 2H),

4.48–4.43 (m, 3H), 3.75 (dd, *J* = 6.4, 3.6 Hz, 1H), 3.13–3.06 (m, 6H), 2.14–1.96 (m, 2H), 1.77–1.35 (m, 4H).

2S-(1RS-benzyloxy-hex-5-enyl)-2,3-dihydro-1,4-benzodioxine (**6**)

A suspension of pyrocatechol (2.96 g, 26.84 mmol) and potassium carbonate (11.13 g, 80.62 mmol) in DMF (65 mL) was stirred for 30 min. Then, a solution of **5** (10.91 g, 26.84 mmol) in DMF (65 mL) was added dropwise to the mixture. The reaction was stirred at room temperature until TLC indicated the disappearance of the starting material. Afterward, the solvent was evaporated in vacuo, and the crude was dissolved in DCM and washed with a 10% aqueous solution of HCl and brine. The organic phase was dried over anhydrous sodium sulfate, filtered, and evaporated in vacuo. Flash chromatography (cyclohexane/ethyl acetate 90:10) was performed to obtain the pure products **6**.

2*S*-(1*R*-benzyloxy-hex-5-enyl)-2,3-dihydro-1,4-benzodioxine (2.70 g, 39,5% calculated considering as 100% the sum of the purified diastereomers), colorless oil: TLC (cyclohexane/isopropyl ether 90:10) R_f = 0.63 $[\alpha]_D^{25}$ ($CHCl_3$, c = 1) + 14.03, ^{1}H NMR (C_6D_6) δ 7.32 (m, 2H), 7.27–7.24 (m, 2H), 7.22–7.18 (m, 1H), 7.17–7.14 (m, 1H), 7.13–7.10 (m, 1H), 6.93–6.83 (m, 2H), 5.83 (ddt, *J* = 16.9, 10.2, 6.7 Hz, 1H), 5.17–5.03 (m, 2H), 4.51 (d, *J* = 11.6 Hz, 1H), 4.48 (d, *J* = 11.6 Hz, 1H), 4.21 (dd, *J* = 11.4, 2.4 Hz, 1H), 4.13 (dd, *J* = 11.4, 6.8 Hz, 1H), 4.00 (ddd, *J* = 12.8, 6.8, 2.4 Hz, 1H), 3.60 (ddd, *J* = 12.8, 6.3, 3.9 Hz, 1H), 2.0 (q, *J* = 7.0 Hz, 2H), 1.72–1.37 (m, 4H). ^{1}H NMR ($CDCl_3$) δ 7.43–7.30 (m, 5H), 6.96–6.83 (m, 4H), 5.83 (ddt, *J* = 16.9, 10.2, 6.7 Hz, 1H), 5.10–4.94 (m, 2H), 4.67 (s, 2H), 4.38 (dd, *J* = 10.6, 1.5 Hz, 1H), 4.24–4.13 (m, 2H), 3.74 (dd, *J* = 11.1, 5.6 Hz, 1H), 2.11 (q, *J* = 7.2 Hz, 2H), 1.77–1.71 (m, 2H), 1.71–1.60 (m, 1H), 1.59–1.49 (m, 1H). ^{13}C-NMR (75 MHz, $CDCl_3$): 147.51, 146.65, 139.00, 137.93, 128.32, 128.18, 217.85, 121.60, 120.86, 117.89, 117.49, 115.35, 79.32, 78.08, 72.09, 66.77, 35.46, 29.25, 23.54. Elemental Analysis Calc (%) for $C_{21}H_{24}O_3$: C, 77.75; H, 7.46. Found (%): C, 77.77; H, 7.47.

2*S*-(1*S*-benzyloxy-hex-5-enyl)-2,3-dihydro-1,4-benzodioxine (1.76 g, 60,5% calculated considering as 100% the sum of the purified diastereomers), colorless oil: TLC (cyclohexane/isopropyl ether 90:10) R_f = 0.54 $[\alpha]_D^{25}$ ($CHCl_3$, c = 1) + 5.10, ^{1}H NMR (C_6D_6) δ 7.35–7.30 (m, 2H), 7.27–7.23 (m, 2H), 7.23–7.17 (m, 1H), 7.17–7.11 (m, 2H), 6.95–6.78 (m, 2H), 5.81 (ddt, *J* = 16.9, 10.2, 6.7 Hz, 1H), 5.17–5.01 (m, 2H), 4.50 (d, *J* = 11.6 Hz, 1H), 4.39 (d, *J* = 11.6 Hz, 1H), 4.16 (ddd, *J* = 8, 4.8, 2.2, 1H), 4.12 (dd, *J* = 11.3, 2.2 Hz, 1H), 3.94 (dd, *J* = 11.3, 8.0 Hz, 1H), 3.52 (ddd, *J* = 8.5, 4.8, 4.1, 1H), 2.00 (q, *J* = 7.9 Hz, 2H), 1.69–1.33 (m, 4H). ^{1}H NMR ($CDCl_3$) δ 7.41–7.28 (m, 5H), 6.97–6.79 (m, 4H), 5.79 (ddt, *J* = 16.9, 10.2, 6.7 Hz, 1H), 5.09–4.93 (m, 2H), 4.75–4.56 (m, 2H), 4.32–4.20 (m, 2H), 4.16–4.03 (m, 1H), 3.68 (dt, *J* = 9.1, 4.6 Hz, 1H), 2.08 (dd, *J* = 14.1, 6.9 Hz, 2H), 1.79–1.39 (m, 4H). ^{13}C-NMR (75 MHz, $CDCl_3$): 147.64, 146.86, 139.50, 138.41, 128.22, 128.08, 127.45, 122.41, 120.36, 117.79, 117.52, 115.45, 78.22, 78.08, 72.09, 68.82, 35.56, 29.15, 23.57. Elemental Analysis Calc (%) for $C_{21}H_{24}O_3$: C, 77.75; H, 7.46. Found (%): C, 77.76; H, 7.47.

4. Conclusions

In conclusion, the combination of molecular modeling and NMR experiments has proven to be a powerful and effective approach for assigning the configuration of the newly formed stereocenter. The synergy between computational simulations and experimental techniques has provided a comprehensive understanding of the spatial arrangement of atoms in the molecule, allowing for the determination of stereochemical details. Thus, we assigned the *R* configuration to the diastereomer with higher R_f, i.e., 2*S*-(1*R*-benzyloxy-hex-5-enyl)-2,3-dihydro-1,4-benzodioxine and the *S* configuration to the one with lower R_f, i.e, 2*S*-(1*S*-benzyloxy-hex-5-enyl)-2,3-dihydro-1,4-benzodioxine.

Supplementary Materials: Figure S1: ^{1}H-NMR spectrum of compound (2*S*, 1*R*)-**6** in C_6D_6; Figure S2: 2D-NOESY of compound (2*S*, 1*R*)-**6**; Figure S3: ^{1}H-NMR spectrum of compound (2*S*, 1*S*)-**6** in C_6D_6; Figure S4: 2D-NOESY of compound (2*S*, 1*S*)-**6**; Figure S5: ^{1}H-NMR spectrum of compound (2*S*, 1*R*)-**6** in $CDCl_3$; Figure S6: ^{13}C-NMR spectrum of compound (2*S*, 1*R*)-**6** in $CDCl_3$; Figure S7 ^{1}H-NMR spectrum of compound (2*S*, 1*S*)-**6** in $CDCl_3$; Figure S8: ^{13}C-NMR spectrum of compound (2*S*, 1*S*)-**6** in $CDCl_3$; Figure S9: Distances between 1′H and 2H and 3H of compound (2*S*, 1*R*)-**6**; Figure S10: Distances between 1′H and 2H and 3H of compound (2*S*, 1*S*)-**6**; Figure S11: ^{1}H-NMR spectrum of

compound (2*S*, *1R*)-**6** in $CDCl_3$ and ^{1}H-NMR spectrum of compound (2*S*, *1R*)-***6*** in C_6D_6; Figure S12: ^{1}H-NMR spectrum of compound (2*S*, *1S*)-**6** in $CDCl_3$ and ^{1}H-NMR spectrum of compound (2*S*, *1S*)-***6*** in C_6D_6.

Author Contributions: Conceptualization, L.F.; methodology, L.F. and A.A.; investigation, A.A.; resources, L.F.; data curation, A.A. and L.F.; writing—original draft preparation, A.A. and L.F.; writing—review and editing, L.F.; supervision, L.F.; project administration, L.F.; funding acquisition, L.F. All authors have read and agreed to the published version of the manuscript.

Funding: This research received no external funding.

Data Availability Statement: The data are contained within the article.

Conflicts of Interest: The authors declare no conflicts of interest.

Abbreviations

tetrahydrofuran (THF), methanol (MeOH), dichloromethane (DCM), dimethylformamide (DMF), thin layer chromatography (TLC), retention factor (R_f).

References

1. Sun, J.; Wang, S.; Sheng, G.-H.; Lian, Z.-M.; Liu, H.-Y.; Zhu, H.-L. Synthesis of Phenylpiperazine Derivatives of 1,4-Benzodioxan as Selective COX-2 Inhibitors and Anti-Inflammatory Agents. *Bioorg Med. Chem.* **2016**, *24*, 5626–5632. [CrossRef] [PubMed]
2. Nelson, W.L.; Wennerstrom, J.E.; Dyer, D.C.; Engel, M. Absolute Configuration of Glycerol Derivatives. 4. Synthesis and Pharmacological Activity of Chiral 2-Alkylaminomethylbenzodioxans, Competitive .Alpha.-Adrenergic Antagonists. *J. Med. Chem.* **1977**, *20*, 880–885. [CrossRef] [PubMed]
3. Campbell, S.F.; Davey, M.J.; Hardstone, J.D.; Lewis, B.N.; Palmer, M.J. 2,4-Diamino-6,7-Dimethoxyquinazolines. 1. 2-[4-(1,4-Benzodioxan-2-Ylcarbonyl)Piperazin-1-Yl] Derivatives as .Alpha.1-Adrenoceptor Antagonists and Antihypertensive Agents. *J. Med. Chem.* **1987**, *30*, 49–57. [CrossRef] [PubMed]
4. Scott, L.J. Eliglustat: A Review in Gaucher Disease Type 1. *Drugs* **2015**, *75*, 1669–1678. [CrossRef] [PubMed]
5. Kong, Z.; Sun, D.; Jiang, Y.; Hu, Y. Design, Synthesis, and Evaluation of 1, 4-Benzodioxan-Substituted Chalcones as Selective and Reversible Inhibitors of Human Monoamine Oxidase B. *J. Enzyme Inhib. Med. Chem.* **2020**, *35*, 1513–1523. [CrossRef] [PubMed]
6. Wang, S.; Haikarainen, A.; Pohjakallio, A.; Sipilä, J.; Kaskinoro, J.; Juhila, S.; Jalava, N.; Koskinen, M.; Vesajoki, M.; Kumpulainen, E.; et al. 2,3-Dihydrobenzo-Dioxine Piperidine Derivatives as Potent and Selective A2c Antagonists. *Bioorganic Med. Chem. Lett.* **2022**, *69*, 128783. [CrossRef]
7. Fumagalli, L.; Bolchi, C.; Bavo, F.; Pallavicini, M. Crystallization-Based Resolution of 1,4-Benzodioxane-2-Carboxylic Acid Enantiomers via Diastereomeric 1-Phenylethylamides. *Tetrahedron Lett.* **2016**, *57*, 2009–2011. [CrossRef]
8. Fumagalli, L.; Pallavicini, M.; Budriesi, R.; Gobbi, M.; Straniero, V.; Zagami, M.; Chiodini, G.; Bolchi, C.; Chiarini, A.; Micucci, M.; et al. Affinity and Activity Profiling of Unichiral 8-Substituted 1,4-Benzodioxane Analogues of WB4101 Reveals a Potent and Selective A1B-Adrenoceptor Antagonist. *Eur. J. Med. Chem.* **2012**, *58*, 184–191. [CrossRef] [PubMed]
9. Artasensi, A.; Angeli, A.; Lammi, C.; Bollati, C.; Gervasoni, S.; Baron, G.; Matucci, R.; Supuran, C.T.; Vistoli, G.; Fumagalli, L. Discovery of a Potent and Highly Selective Dipeptidyl Peptidase IV and Carbonic Anhydrase Inhibitor as "Antidiabesity" Agents Based on Repurposing and Morphing of WB-4101. *J. Med. Chem.* **2022**, *65*, 13946–13966. [CrossRef] [PubMed]
10. Bothner-By, A.A. Geminal and Vicinal Proton-Proton Coupling Constants in Organic Compounds. In *Advances in Magnetic and Optical Resonance*; Elsevier: Amsterdam, The Netherlands, 1965; pp. 195–316.
11. Karplus, M. Vicinal Proton Coupling in Nuclear Magnetic Resonance. *J. Am. Chem. Soc.* **1963**, *85*, 2870–2871. [CrossRef]
12. Schmid, C.R.; Bryant, J.D. D-(R)-Glyceraldehyde Acetonide. *Org. Synth.* **1995**, *72*, 6. [CrossRef]
13. Osawa, E.; Ouchi, T.; Saito, N.; Yamato, M.; Lee, O.S.; Seo, M.-K. *Critical Evaluation of an Empirically Modified Karplus Equation*; Wiley Online Library: Hoboken, NJ, USA, 1992; Volume 30.
14. Pedretti, A.; Mazzolari, A.; Gervasoni, S.; Fumagalli, L.; Vistoli, G. The VEGA Suite of Programs: An Versatile Platform for Cheminformatics and Drug Design Projects. *Bioinformatics* **2021**, *37*, 1174–1175. [CrossRef] [PubMed]

Disclaimer/Publisher's Note: The statements, opinions and data contained in all publications are solely those of the individual author(s) and contributor(s) and not of MDPI and/or the editor(s). MDPI and/or the editor(s) disclaim responsibility for any injury to people or property resulting from any ideas, methods, instructions or products referred to in the content.